

Water Resources Research

RESEARCH ARTICLE

10.1002/2015WR018236

Kev Points:

- Additional applications of the cosmic ray neutron method can be explored using neutron modeling
- A method to align and make measured and modeled neutron intensities comparable is proposed
- The methodology is validated by modeling measured thermal and fast neutron profiles

Correspondence to:

M. Andreasen, mie.andreasen@ign.ku.dk

Citation:

Andreasen, M., K. H. Jensen, M. Zreda, D. Desilets, H. Bogena, and M. C. Looms (2016), Modeling cosmic ray neutron field measurements, *Water Resour. Res.*, *52*, 6451–6471, doi:10.1002/2015WR018236.

Received 13 OCT 2015 Accepted 24 JUL 2016 Accepted article online 29 JUL 2016 Published online 25 AUG 2016

Modeling cosmic ray neutron field measurements

Mie Andreasen¹, Karsten H. Jensen¹, Marek Zreda², Darin Desilets³, Heye Bogena⁴, and Majken C. Looms¹

¹Department of Geosciences and Natural Resource Management, University of Copenhagen, Copenhagen, Denmark, ²Department of Hydrology and Water Resources, University of Arizona, Tucson, Arizona, ³Hydroinnova LLC, Albuquerque, New Mexico, ⁴Agrosphere Institute (IBG-3), Forschungszentrum Juelich GmbH, Juelich, Germany

Abstract The cosmic ray neutron method was developed for intermediate-scale soil moisture detection, but may potentially be used for other hydrological applications. The neutron signal of different hydrogen pools is poorly understood and separating them is difficult based on neutron measurements alone. Including neutron transport modeling may accommodate this shortcoming. However, measured and modeled neutrons are not directly comparable. Neither the scale nor energy ranges are equivalent, and the exact neutron energy sensitivity of the detectors is unknown. Here a methodology to enable comparability of the measured and modeled neutrons is presented. The usual cosmic ray soil moisture detector measures moderated neutrons by means of a proportional counter surrounded by plastic, making it sensitive to epithermal neutrons. However, that configuration allows for some thermal neutrons to be measured. The thermal contribution can be removed by surrounding the plastic with a layer of cadmium, which absorbs neutrons with energies below 0.5 eV. Likewise, cadmium shielding of a bare detector allows for estimating the epithermal contribution. First, the cadmium difference method is used to determine the fraction of thermal and epithermal neutrons measured by the bare and plastic-shielded detectors, respectively. The cadmium difference method results in linear correction models for measurements by the two detectors, and has the greatest impact on the neutron intensity measured by the moderated detector at the ground surface. Next, conversion factors are obtained relating measured and modeled neutron intensities. Finally, the methodology is tested by modeling the neutron profiles at an agricultural field site and satisfactory agreement to measurements is found.

1. Introduction

Important processes like evapotranspiration, infiltration, and overland flow are moisture dependent. Soil moisture may vary considerable in space and accurate time series of intermediate-scale (hundreds of meters) soil moisture estimates is highly relevant and valuable for validation and calibration of catchment-scale hydrological and climatological models used for water resource management and decision making [Western et al., 2002]. Soil measurements at a scale comparable to the resolution of many of these models can be determined using the cosmic ray neutron detector [Zreda et al., 2008, 2012]. The potential of neutron detectors of additional applications is wide and may accommodate hydrological studies as well as other fields of interest. Applications may include detection of biomass, canopy interception, soil organic matter and snow, and may furthermore set the base for the advancement of the soil moisture estimation method. Especially, this will be true at field sites characterized by these features and processes (e.g., forest). A canopy interception estimation method would be valuable as the canopy interception loss in forests may form a major part of the total evapotranspiration [Ringgaard et al., 2014]. The variable is dependent on many factors (e.g., weather, climate, forest structure, tree type, and size) and may therefore vary considerably both temporally and spatially. The classic methods for canopy interception estimation are uncertain and only applicable at small scale [Dunkerley, 2000], and an intermediate-scale method may set the base for improved evapotranspiration estimates in forests. Different disciplines would gain from a method capable of quantifying intermediate-scale biomass as the forest forms an important resource for renewable energy and timber production. Afforestation is also used as climate change mitigation as carbon is stored in the biomass at tree growth. Biomass estimation from allometric models is the most typical method [Jenkins et al., 2003], but is expensive in man-

© 2016. American Geophysical Union. All Rights Reserved.

hours, especially when larger areas are considered and an estimate of seasonal/annually tree growth is required.

Above the ground surface, the neutron intensity (eV range) is dependent on the elemental composition and density of the surrounding air and soil matrix. The components are stable, quasi-stable or dynamic, resulting in varying neutron intensity over time. The intensity of moderated neutrons is inversely correlated with hydrogen present at and near the land surface [Zreda et al., 2008]. Using the cosmic ray neutron method, soil moisture can be estimated in the top decimeters of soil and over a horizontal footprint of hectometers [Desilets and Zreda, 2013; Köhli et al., 2015]. Several studies have found that cosmic ray neutron-derived soil moisture values agree with independent area average soil moisture measurements obtained from distributed-sensor networks or gravimetric soil sampling for various types of ecosystems and land covers, e.g., semiarid field sites in southern Arizona, USA [Zreda et al., 2008, 2012; Franz et al., 2012a], humid field sites in northern and western Germany [Rivera Villarreyes et al., 2013; Bogena et al., 2013; Baatz et al., 2014], and at various field sites in Australia [Hawdon et al., 2014]. Furthermore, soil moisture at a scale more suitable for validation and calibration of hydrological catchment models and remotely sensed products have been mapped using the cosmic ray rover in southern Arizona, USA [Chrisman and Zreda, 2013], Oklahoma, USA [Dong et al., 2014], and eastern Nebraska, USA [Franz et al., 2015]. Moreover, the cosmic ray rover has been used for validating the universal calibration function [Franz et al., 2013b] at field locations of various environmental settings and land covers in Australia [McJannet et al., 2014].

Hydrogen is present in several other pools of interest for hydrology besides soil moisture, including atmospheric water vapor, snow, canopy interception, biomass, lattice water, and soil organic matter [Ochsner et al., 2013]. Franz et al. [2013a] found the measured cosmic ray neutron intensity to be lower at field sites with extensive forest covers. The effect of biomass water on the intensity of moderated neutrons was assessed in a pine forest in Arizona, USA, and a maize field in lowa, USA, by independently quantifying all other pools of hydrogen within the footprint using the framework presented in Franz et al. [2013b]. Recently, correction functions to account for aboveground biomass have been suggested [Baatz et al., 2015; Heidbüchel et al., 2015].

Quantifying additional hydrogen pools solely from measured cosmic ray neutron intensities is challenging. The hydrogen pools are distributed both above and below ground (i.e., tree trunks, foliage, soil moisture, and intercepted precipitation within a forest) and these are often also subject to dynamic behavior. Forest vegetation may be assumed to be quasi-static, while canopy interception, soil moisture, and snow is dynamic due to varying meteorological conditions such as precipitation, evaporation, sublimation, and melting.

While there are potentially several unknowns in the system, there are also potentially several ways that neutron intensity can vary in response to these unknowns. These variations include changes in the neutron energy spectrum and changes in the altitude profile of neutron intensity, or a combination of both [Desilets et al., 2010]. Thermal neutrons are like epithermal neutrons sensitive to hydrogen and are therefore also relevant to consider for hydrological applications. In terms of the physical properties, thermal and epithermal neutrons are very different. This may cause the signal of a specific variable to be different for the two energy ranges, and the signals may provide valuable information both separately and jointly. Procedures to separate and quantify the hydrogen pools can potentially be based on measurements of neutron intensity alone, thereby eliminating the need for tedious and labor intensive surveys using independent methods. Desilets et al. [2010] stressed the potential of estimating soil moisture and biomass simultaneously using neutron detectors installed above and below the forest canopy. The effect of separate hydrogen pools on the neutron intensity profiles is poorly constrained by experiment. This is in part because multiple processes can occur simultaneously (e.g., drying/wetting of soil and canopy), and because the detected neutron intensities from conventional small-size cosmic ray neutron detectors are noisy at short time scales. For example, an appropriate time scale for canopy interception is subhourly to hourly, and this effect is difficult to measure with adequate precision using neutron detectors.

Modeling neutron transport at specific field locations and at different environmental settings can serve as an essential tool to isolate the effect of different types of hydrogen pools. A representative model mimicking measured neutron intensities can be used to evaluate the effect of different elements and hydrogen pools on thermal and epithermal neutrons by varying the governing variables and parameters. This may

be used to improve the method for soil moisture estimation as the signal of the other influencing components on the thermal and epithermal neutron intensity can be removed. This will especially be relevant for neutron intensity detection at forest field sites. Here multiple hydrogen pools of considerable sizes affect the neutron intensity signal resulting in cosmic ray soil moisture estimates of higher uncertainties [Bogena et al., 2013; Franz et al., 2013a]. Moreover, modeling neutron transport may set the base for the development of additional applications for the cosmic ray neutron intensity method. This includes methods to estimates canopy interception, biomass, soil organic matter and snow, and involves thermal and epithermal neutrons at multiple height levels above the ground surface. In the literature, neutron flux modeling within the field of hydrology has mostly been focused on: (1) development of a standard relationship between neutron intensity and soil moisture, known as the N₀ method [Desilets et al., 2010]. (2) Investigation of the detector footprint [Desilets and Zreda, 2013; Köhli et al., 2015]. (3) Determination of a universal calibration function [Franz et al., 2013b]. (4) Development of a water vapor correction model [Rosolem et al., 2013]. (5) Investigation on the effect of snow cover on the cosmic ray neutron intensity [Zweck et al., 2013]. (6) Examination of the ground surface thermal and epithermal neutron intensity response to hydrogen [McJannet et al., 2014]. Modeling of neutron intensity measurements from a particular field location using site specific soil chemistry has only been conducted for the development of the universal calibration function [Franz et al., 2013b]. However, validation of neutron transport modeling was not performed in the study.

To enable model validation, the energy ranges of the measured and modeled neutron intensities need to be aligned. Specific energy ranges of thermal (0–0.5 eV (electron Volt) by *Zweck et al.* [2013] and *McJannet et al.* [2014]) and epithermal neutrons (10–1000 eV by *Desilets and Zreda* [2013] and *McJannet et al.* [2014]) are modeled, while the exact energy sensitivity of the bare and the moderated neutron detector is not well known. *McJannet et al.* [2014] found a better agreement to ground surface measurements of the moderated detector when the modeled neutron intensity consisted of 30% thermal neutrons and 70% epithermal neutrons, relative to 100% epithermal neutrons. However, the suggested fraction of thermal and epithermal neutrons measured by the moderated detector is based on guesses. The response of the neutron detector may vary with height above the ground, location and detector and a more thorough examination of both the bare and the moderated detector is necessary. Studies of the response of the neutron detectors are found in the literature within the field of radiation protection and fundamental science on cosmic radiation. For example, the neutron flux and its energy distribution for neutrons at energies 10^{-10} MeV to 100 GeV ($1 \text{ eV} = 1.6 \times 10^{-19} \text{ J}$) has been examined with great detail using measurements (neutron spectrometer) and particle modeling [*Clem and Dorman*, 2000; *Goldhagen et al.*, 2002; *Gordon et al.*, 2004; *Rühm et al.*, 2009].

Furthermore, both the measured and modeled neutron intensities are relative, not absolute. Measured intensities depend on the specific neutron detector characteristics such as size, type and pressure of ionization gas, and thickness of moderating material as well as the geographical location of the detector both with respect to elevation (atmospheric pressure) and geomagnetic cutoff rigidity [Desilets and Zreda, 2001, 2003; Desilets et al., 2006; Zreda et al., 2012]. On the other hand, modeled intensities are the ratio of counts to the number of particles released at the upper boundary of the numerical model [Pelowitz, 2011].

In this paper, we develop a method to make measured and modeled neutron intensities directly comparable and thus providing a possibility to expand the use of the cosmic ray neutron method for additional hydrological applications. The method involves separating the thermal and epithermal neutron intensities from raw measurements. Pure thermal and epithermal neutron intensities are acquired by removing the epithermal neutron contribution and the thermal neutron contribution from the bare and the moderated detector, respectively. Model-to-measurements conversion factors are determined to allow for a direct comparison of measurements and modeling. We consider our study as a first step toward merging measurements and modeling. Therefore, we recommend further studies and technical developments in order to advance the method and reduce the uncertainties.

Neutron energy correction models are determined by applying the cadmium difference method [Knoll, 2010] for three field locations (Gludsted Plantation and Ringkøbing Fjord, western Denmark, and Wüstebach Test Site, western Germany) in order to obtain thermal and epithermal neutron intensities from bare and moderated detectors. We evaluate the impact of using the deduced neutron energy correction models on

measurements from Gludsted Plantation. To enable future investigation on the potential of estimating canopy interception and biomass using neutron detectors above and below the forest canopy, the neutron energy correction models have to be applied for neutron intensity at multiple height levels. Therefore, continuous time series of cosmic ray neutron intensity measurements (2013–2015) at two heights, as well as neutron profiles with temporary neutron detection (hours) at multiple height levels from the ground surface to 35 m height are used. The neutron profiles of the Gludsted Plantation were detected during two field campaigns (November 2013 and March 2014).

Model-to-measurements conversion factors are found by relating measured and modeled neutron intensities over reference conditions (100% water) in order to enable modeling of measured neutron intensities. Finally, the proposed methodology is demonstrated by comparing measured and modeled neutron intensity profiles for an agricultural site in western Denmark.

2. Field Sites

Data from four field locations are used in this study (Figure 1). The Gludsted Plantation, the Ringkøbing Fjord, and the Voulund Farmland are situated in western Denmark in the Skjern River catchment and form part of the Danish hydrological observatory (HOBE) [Jensen and Illangasekare, 2011]. The Wüstebach Test Site is a subcatchment of the River Rur basin in the western part of Germany and is part of the TERENO Eifel/Lower Rhine Observatory [Zacharias et al., 2011]. Details of the individual sites are given below.

2.1. Gludsted Plantation

The Gludsted Plantation is a forest field site located within Denmark's largest coniferous forest plantation (approximately 3500 ha) (Figure 1). The field site is located on a glacial outwash plain with flat terrain and sandy stratified soils (56°04′24″N 9°20′06″E). The elevation is approximately 50 m above sea level. The plantation consists primarily of rows of Norway spruce (Picea abies). Soils are nutrient depleted with a low decomposition rate, resulting in a thick and continuous organic-rich litter layer of 7–10 cm on the forest floor. The dry aboveground biomass within the footprint of the cosmic ray neutron detector was estimated to be around 100 t/ha using Light Detection and Ranging images (LiDAR) from 2006 and 2007 [Nord-Larsen and Schumacher, 2012]. Measurements of cosmic ray neutron intensity at multiple heights were made from a 38 m high tower.

2.2. Ringkøbing Fjord

The Ringkøbing Fjord is a shallow brackish lagoon located in the western part of Denmark around 60 km west of the Gludsted Plantation (Figure 1). It covers an area of about 300 km² and is fed by saltwater from the North Sea and freshwater from streams and groundwater discharge [Kinnear et al., 2013]. The inflow of seawater is controlled using a slushing system at the inlet to Ringkøbing Fjord and the salinity is at a detection station in the center of the fjord measured to be between 6 and 15 ppm [Haider et al., 2015]. A water sample was collected approximately 500 m from the eastern shoreline (55°59′31″N 8°18′04″E) on 30 June 2014. The chemical composition of the brackish water was determined using Atomic Absorption Spectroscopy and Ion Chromatography (Table 1).

2.3. Voulund Farmland

The Voulund Farmland (56°02′14″N 9°09′38″E) is an agricultural field site located in the central part of Jutland (Figure 1). The field site, situated approximately 10 km west of the Gludsted Plantation, is located on the same outwash plain as described above approximately 57 m above sea level. The soil is a spodosol consisting of coarse sand with 25 cm thick organic-rich topsoil.

Soil samples were collected at 108 locations on 23 September 2015 following the scheme of *Franz et al.* [2012a] and area average soil moisture and dry bulk density were calculated for the top 20 cm of the soil. The soil organic carbon was determined for a mixed sample of 108 soil samples collected on 29 August 2013. Further, major element chemical composition of the topsoil was determined using the X-ray Fluorescence Analyzer (Table 1). The sensitivity of rare earth elements on thermal and epithermal neutron intensity was determined from modeling using elements with considerable cross sections. The analysis suggested the element Gadolinium (Gd) to be an important sink for thermal neutrons due to the high thermal neutron absorption cross section of around 49,000 barns (1 barn = 10^{-24} cm²). The Gd concentration was found to

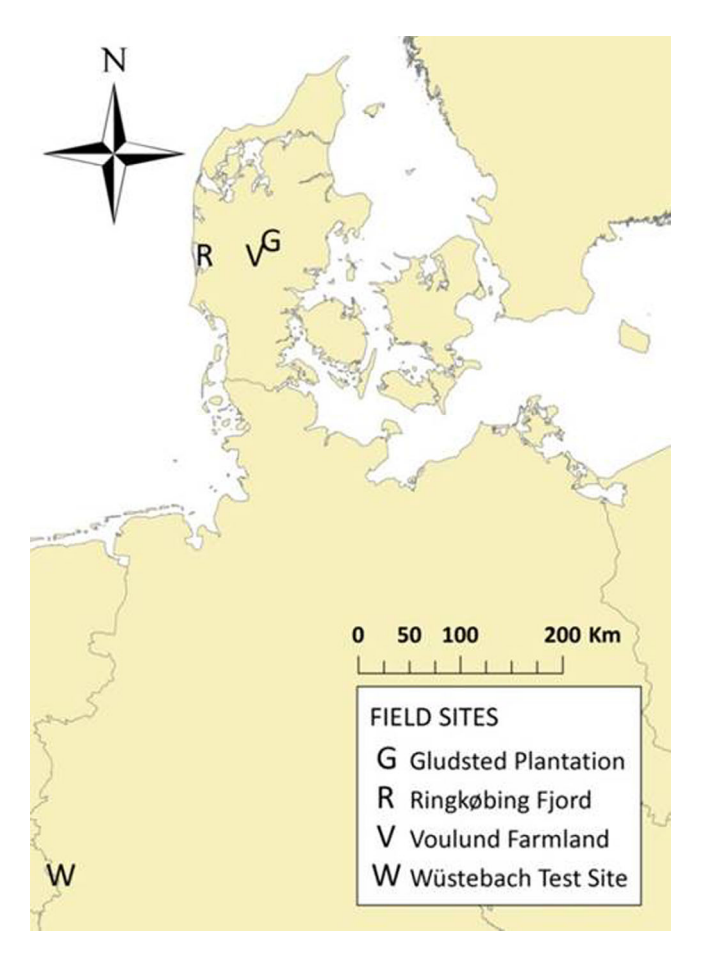


Figure 1. Map showing the locations of the four field sites.

be 0.51 ppm in the topsoil for a location situated 15–20 km from the Voulund Farmland field site [Salminen et al., 2005]. The site is located at the same outwash material and is assumed to be representative of the Voulund Farmland field site.

Measurements of cosmic ray neutron intensity at several heights were conducted from a 12 m high tower.

2.4. Wüstebach Test Site

The Wüstebach experimental test site (50°30′N, 6°19′E) is a forest field site located approximately 595–625 m above sea level with an average slope of 3.6% (Figure 1). The vegetation consists primarily (90%) of Norway spruce (Picea abis) planted in 1946. From tree allometry, the dry aboveground biomass was estimated to be around 300 t/ha [*Baatz et al.*, 2015]. The soil thickness ranges between approximately 1 and 2 m and the soil texture is loamy silt. The soil is overlaid by a litter layer with a thickness between 0.5 and 14 cm [*Bogena et al.*, 2015]. Measurements of cosmic ray neutron intensities at different heights are made possible from a 38 m high meteorological tower. Since February 2014, neutron intensities are measured using bare and moderated detectors mounted at 1.5 and 30 m height, respectively.

3. Cosmic Ray Neutron Methodology

3.1. Terminology

The following terminology is used for the neutron energy ranges representative of different behaviors and sensitivities:

1. Thermal neutrons: energies in the range of 0-0.5 eV.

Table 1. The Chemical Composition of the Water for the Saltwater, the Freshwater (at 10°C) and the Ringkøbing Fjord Models, As Well As for the Soil of the Voulund Farmland and the Pure Silica Soil (SiO₂) Models^a

| | | | · - | | | |
|--------------------------|-------------------------------------|-------------------------------|--------------------------------------|-----------------------------|--|--|
| _ | Saltwater (mol/cm ³) | Ringkøbing Fjord (mol/cm³) | Freshwater (mol/cm ³) | | Voulund Farmland (mol/cm ³) | Pure SiO ₂ (mol/cm ³) |
| Н | 0.1098 ^b | 0.1112 ^c | 0.1110 ^b | Н | 0.0038 ^c | 0.0179 ^c |
| 0 | 0.0550 ^b | 0.055 ^c | 0.0555 ^b | 0 | 0.0448 ^c | 0.0547 ^{c,d} |
| Na | 4.97E-4 ^b | 1.36E-4 ^c | | Si | 0.0199 ^c | 0.0229 ^d |
| Mg | 5.65E-5 ^b | 1.39E-5 ^c | | Al | 0.0016 ^c | |
| Ca | 1.10E-5 ^b | 3.45E-6 ^c | | Р | 1.04E-4 ^c | |
| K | 1.09E-5 ^b | 6.39E-7 ^c | | K | 2.89E-4 ^c | |
| Cl | 5.80E-4 ^b | 1.73E-4 ^c | | Ca | 1.08E-4 ^c | |
| S | 3.00E-5 ^b | 7.40E-6 ^c | | Ti | 5.46E-5 ^c | |
| C | 2.46E-6 ^b | | | Fe | 2.73E-5 ^c | |
| N | 7.18E-12 ^b | | | C | 0.0023 ^c | |
| P | | 7.46E-7 ^c | | Gd | 4.46E-9 ^d | |
| Br | | 1.46E-7 ^c | | | | |
| F | | 3.50E-7 ^c | | | | |
| Water density (g/cm³) | 1.025 ^e | 1.0125 ^e | 1.00 ^e | Dry bulk density (g/cm³) | 1.472 | 1.472 |

^aStandard chemical composition of seawater and freshwater is used for the saltwater model [Appelo and Postma, 2005] and the freshwater model, respectively, while the chemical composition of the water of the Ringkøbing Fjord was measured. The water density is calculated. The chemical composition, the area average volumetric soil moisture (0.222), and bulk density of the mineral soil at the Voulund Farmland is measured.

- 2. Epithermal neutrons: energies higher than 0.5 eV
- 3. Fast neutrons: energies in the range of 10–1000 eV. Thus, fast neutrons are included in the epithermal neutron energy range.

3.2. Detectors

The CR1000/B and CR2000/B systems of Hydroinnova LLC, Albuquerque, New Mexico, are used for the measurements of cosmic ray neutron intensities. The systems hold a data logger, sensors measuring barometric pressure, relative humidity, and temperature, and two neutron intensity detectors. The first detector is the bare detector (Figure 2a). It consists of a tube filled with boron-10 trifluoride ($^{10}BF_3$) proportional gas at a pressure of 0.6 atm. The $^{10}B(n,\alpha)^TLi$ reaction is very effective in converting thermal neutrons into detectable electrons as the cross section of ^{10}B is high at thermal energies (3840 barns). The cross section decreases rapidly with increasing neutron energy following $1/E_n^{0.5}$ (where E_n is neutron energy) [*Knoll*, 2010]. Thus, the probability of interaction decreases with increasing neutron energy and the measured neutrons are therefore of thermal energies. However, since there is no abrupt cutoff, a small proportion of epithermal neutrons is also detected.

The second detector (referred to as the moderated detector) consists of a 10 BF $_3$ proportional tube (similar to the bare detector) embedded within a 25 mm thick moderator (made from high-density polyethylene, common plastic) (Figure 2c). Neutrons traveling though the moderator will interact with hydrogen atoms of the moderator material and be slowed down by elastic collisions. Neutrons of $E_n > 0.5$ eV are mostly scattered, while the probability of absorption is large for neutrons of $E_n < 0.5$ eV. Regardless of the presence of a moderator, the energy range of the neutrons measured by the proportional tube is always the same. The difference lies in the fact that the neutrons measured by the moderated detector originate from a higher energy range. The neutrons detected by the moderated detector in the CR1000/B and CR2000/B systems are primarily of energies >1 eV, although thermal neutrons may also find their way through the plastic.

As a result of the different properties of thermal and epithermal neutrons (e.g., the mean free path), the footprint of the bare and moderated detector is expected to be different. Previous studies have reported different values of the footprint diameter of the moderated detector based on neutron transport modeling. *Desilets and Zreda* [2013] found a value of 600 m, while *Köhli et al.* [2015] suggested it to be 260–480 m. The footprint of the bare detector has not yet been examined. However, the decrease in thermal neutron intensity to around 100–200 m height is an effect of the air-surface boundary [*Desilets et al.*, 2009, Figure 2] and

^bTable values.

^cMeasurements.

^dAssumed values.

^eCalculated values.

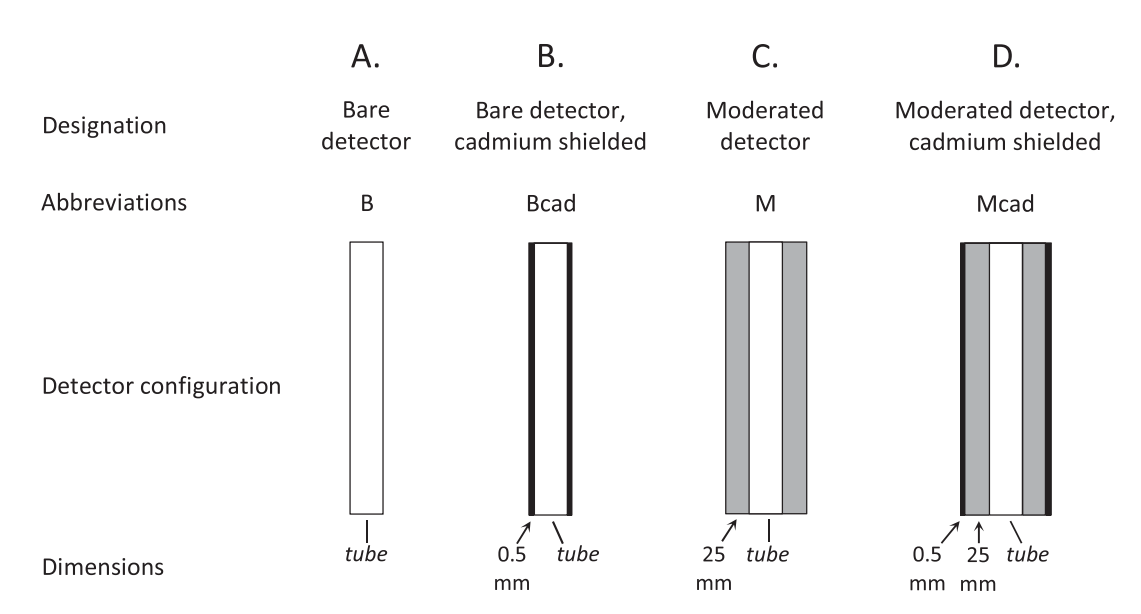


Figure 2. Configuration and dimensions of the neutron detectors: (a) bare detector, (b) cadmium-shielded bare detector, (c) moderated detector (plastic embedded bare detector), and (d) cadmium-shielded moderated detector. The diameter of the ¹⁰BF₃ proportional tube is 50.8 and 76.2 mm for the CR1000/B and CR2000/B detectors, respectively.

may be regarded as an indicator for the footprint of the thermal neutrons. Thus, we expect the footprint of the bare detector to be at a scale of hectometers. Future work should further analyze the footprint of the bare and the moderated detector, both from modeling and field experiments.

Neutron intensities follow a Poisson distribution and therefore Poissonian statistics is the appropriate basis for the computation of uncertainty. The uncertainty of neutron intensity, N, decreases with increasing neutron intensity and the standard deviation equals N^{0.5} [Knoll, 2010]. The neutron count rate of detectors like the CR1000/B and CR2000/B systems depends on the pressure and type of gas within the tube (³He or BF₃), the tube size, and the thickness and material of the moderator. As the CR2000/B detector and embedded tube is larger, it has higher count rates and the relative uncertainty of the measurements is smaller. Since slight variations in the pressure of the BF₃-gas may exist between similar detectors, cross referencing and determination of normalization factors are advisable prior to experiments using multiple detectors [Baatz et al., 2015].

3.3. Cadmium Difference Method

The contribution of thermal and epithermal neutrons measured by the bare and moderated detectors can be determined by applying the cadmium difference method [Knoll, 2010]. The thermal absorption cross section of cadmium is very large (around 3500 barns) for neutron energies below 0.5 eV. The cross section drops sharply with increasing neutron energy and remains low at energies higher than 0.5 eV (around 6.5 barns) [Knoll, 2010; Glasstone and Edlund, 1952]. The neutron energy 0.5 eV is referred to as the cadmium cutoff. Simultaneous neutron intensity detection using noncadmium-shielded and cadmium-shielded neutron detectors reveal the fraction of thermal and epithermal neutrons measured. Here a 0.5 mm thick cadmium foil (purity of 99.85%) was used to filter epithermal neutrons. To verify the effectiveness of this filter, the manufacturer performed a laboratory experiment with a moderated CRS1000-type sensor using a single layer of this foil followed by a double layer, and using a reference detector (without cadmium) to correct for temporal changes in intensity. They reported that the first layer of foil reduced the counting rate by 30%, whereas the second layer reduced the counting rate by only a further 3%. According to the manufacturer, this small additional reduction is likely due to the filtering of neutrons with energies near or just above the effective cadmium cutoff energy.

A schematic of the effect on the measured neutron energy range, when using the cadmium difference method, is presented in Figure 3. The cadmium difference method using both the bare and the moderated detector is described below.

When a bare detector is shielded with cadmium foil (B_{Cad}) (Figure 2b), the thermal neutrons are removed from the measured signal and neutron intensities of epithermal energies are measured (see Figure 3c).

From here on we refer to these detected neutrons as the "epithermal contribution" to the bare detector signal. The thermal neutron intensity (T) (Figure 3e) is calculated by subtracting this epithermal contribution B_{Cad} from the neutron intensity measured by the bare detector (B) (Figure 3a), see equation (1).

$$T=B-B_{Cad} \tag{1}$$

Likewise, a cadmium-shielded moderated detector (M_{Cad}) (see Figure 2d) measures neutrons of epithermal energies (E) (Figure 3d). The difference between the neutron intensity measured by moderated detector (M)

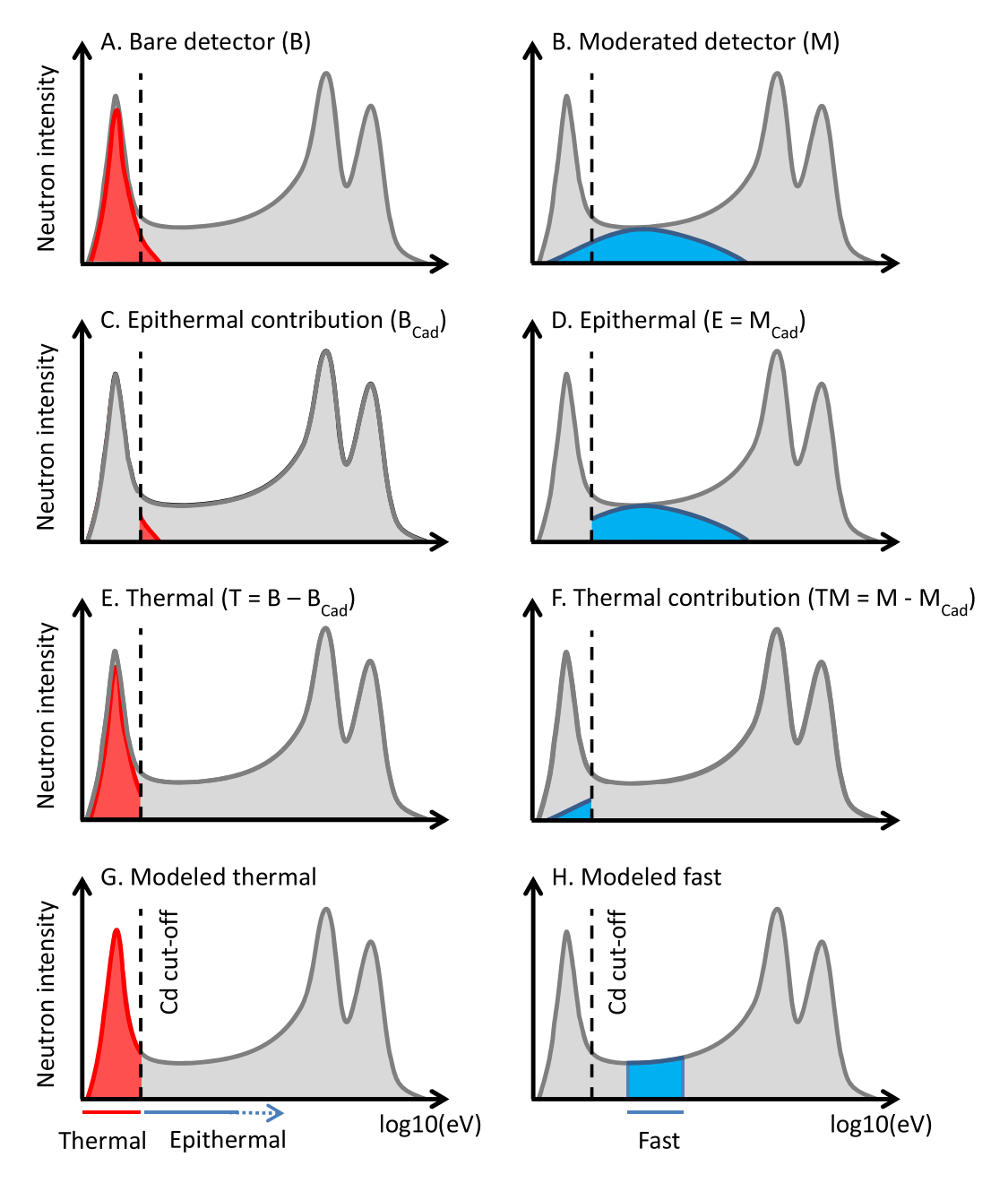


Figure 3. A sketch illustrating the neutron energy spectra (grey) (modified from Köhli et al. [2015]) and the energy range of (a–f) measured and (g and h) modeled neutron intensities. (a) Bare neutron intensity detector. (b) Moderated neutron intensity detector. (c) The epithermal contribution measured by the cadmium-shielded bare detector. (d) The moderated epithermal neutron intensity measured by the cadmium-shielded moderated detector. (e) The thermal neutron intensity computed by subtracting the epithermal contribution (Figure 3c) from measurements with the bare detector (Figure 3a). (f) The thermal contribution computed by subtracting the moderated epithermal neutron intensity (Figure 3d) from moderated measurements (Figure 3b). (g) The energy range of the modeled thermal neutron intensity (set to 0–0.5 eV). (h) The energy range of the modeled fast neutron intensity (set to 10–1000 eV). The cadmium (Cd) cutoff is shown by the vertical dashed line at 0.5 eV.

(Figure 3b) and the cadmium-shielded moderated detector M_{Cad} is from here on referred to as the "thermal contribution" (TM) to the moderated detector (Figure 3f), see equation (2).

$$TM = M - M_{Cad} \tag{2}$$

As a result of applying the cadmium difference method, a well-defined energy range is produced, which facilitates comparison with neutron transport simulations.

3.4. Measurements

In accordance to the standard procedure detailed in *Zreda et al.* [2012], outliers were removed from the neutron intensity data set and measurements by moderated detectors were corrected for the temporal changes in barometric pressure, atmospheric water vapor, and incoming cosmic ray intensity. Despite the closer proximity of the Kiel neutron monitor (Northern Germany) to the field sites, data from the Jungfraujoch neutron monitor (Switzerland) were used for the correction of temporal changes in the incoming neutron intensity. The two data sets have similar patterns and dynamics, and we find the Jungfraujoch neutron monitor more appropriate as the data set is characterized by fewer and shorter data gaps in the time period 2013–2015. Neutron intensities measured by bare detectors were corrected following the same correction scheme, except we chose not to correct for changes in the atmospheric water vapor using the correction for moderated neutrons developed by *Rosolem et al.* [2013]. Preliminary modeling results by the authors and R. Rosolem (personal communication, 2015) suggest that water vapor only has a minor effect on the thermal neutron intensity measured near the land surface. This is in agreement with earlier studies of *Bethe et al.* [1940] and *Lockwood and Yingst* [1956]. However, water vapor corrections might be required for thermal neutron intensities collected high above the ground surface, and future work should address this issue.

Continuous time series measurements and profile measurements were conducted in this study using both bare and moderated detectors. Furthermore, in order to quantify the thermal neutron contribution and the epithermal neutron contribution the cadmium difference method was applied for both types of measurements. The details of the various measurements are presented below.

3.4.1. Continuous Time Series Measurements

Continuous time series measurements were conducted at three sites: the Gludsted Plantation, the Wüstebach Test Site, and the Ringkøbing Fjord.

Since spring of 2013, two CR1000/B systems have been in operation at the Gludsted Plantation. The systems are installed near the ground surface (1.5 m height) and at the canopy surface (27.6 m height), respectively, and data are integrated on a per hour basis. The data logger is installed inside a heated control house with electrical supply placed a few meters from the mast. The measurements of barometric pressure, relative humidity and temperature collected by the CR1000/B system are not used here as the sensors are situated within the data logger. Instead measurements from sensors installed on the mast were used. The cadmium difference method was performed at both heights on 14–25 March 2014, 26–30 June 2014, and 3–8 July 2014. During the first survey, only the moderated detector was covered by the cadmium shield, while both types of detectors were shielded with cadmium during the last two surveys.

At the Wüstebach Test Site, cosmic ray neutron intensity was continuously measured using two CR2000/B systems, each with a bare and a moderated detector. During the periods 28–31 May 2014 and 2–5 June 2014, measurements were collected at the ground surface (1.5 m height) and at the canopy surface (30 m height), respectively. The data loggers were installed next to the detectors and the systems were charged from batteries placed in the container for the data logger. The cadmium difference method was performed at both height levels using both types of detectors. Data were logged every 15 min.

Cosmic ray neutron intensities were measured from a rubber boat anchored in Ringkøbing Fjord during two field campaigns (25–26 March 2014 and 30 June 2014 to 3 July 2014) for a total of 4 days. All four detectors from Gludsted Plantation were used. The detectors were aligned side by side and fixed on the top of the rubber boat approximately 0.5 m above sea level. To protect the electronics from splashes of water, the data loggers were placed in containers at the bottom of the boat along with the batteries. The batteries and the detectors were furthermore placed in each end of the rubber boat were separated by around 1 m to avoid the heavy metals of the batteries to affect the neutron detection. The detectors were separated by approximately 30 cm to prevent interference of the tubes, as moderation of neutrons from one detector can affect the nearby detector.

The cadmium difference method was performed for the moderated detector during the first survey and for both the bare and moderated detector during the second survey. Finally, cross referencing of the four detectors was performed by simultaneously measuring with the detectors without the cadmium shield for a period of time. Normalization factors were thereby obtained for all detectors.

3.4.2. Profile Measurements

At the Gludsted Plantation, profiles were measured at approximately 5 m increments from the ground surface to 35 m height above the ground on 25–26 November 2013 and 12–14 March 2014 using the CR1000/B systems used for the continuous measurements. The measurements were collected with a 10 min time resolution. Due to the considerable drop in thermal neutron intensity with height above the ground surface, the measurement time was increased at each height to keep the measurement uncertainty at a consistent and low level. Close to sea level (approximately 50 m elevation), neutron intensities are generally low and collecting a profile took 2–3 days. The two profiles were therefore measured during stable weather conditions to minimize any effects of changing weather on neutron intensities. An epithermal neutron intensity profile was collected in March 2014 using a cadmium-shielded moderated detector.

Neutron intensity profiles were collected at the Voulund Farmland using one of the CR1000/B systems normally installed at the Gludsted Plantation. The data logger of the system was placed inside a heated control house with electrical supply placed a few meters from the mast. Measurements of barometric pressure, relative humidity, and temperature for correction of the neutron intensity were obtained from sensors installed on the mast. Neutron intensities profiles were detected on 22 September 2015 and again on 23 September 2015 at two and three height levels, respectively. On 22 September, neutron intensity was measured at 1.5 and 10.75 m height above the ground surface. An extra measurement point at 6 m above the ground surface was added to the neutron profile recorded on 23 September. The weather was stable with no precipitation during the 2 days of profile measurements and the soil moisture is assumed to be similar. Data were logged every 10 min.

3.5. Cosmic Ray Neutron Modeling

The Monte Carlo N-Particle Extended (MCNPX) radiation transport code [*Pelowitz*, 2011] is the most commonly used neutron transport model within the field of hydrology [*Desilets et al.*, 2010; *Desilets and Zreda*, 2013; *Franz et al.*, 2013b; *Rosolem et al.*, 2013; *Zweck et al.*, 2013]. Here both the MCNPX model code and the Monte Carlo N-Particle transport code version 6 (MCNP6) were used. The MCNP6 model code is a merger of the MCNPX model code and the Monte Carlo N-Particle Transport code version 5 (MCNP5), and all new advances and code capabilities are developed and released in this new code version [*Goorley et al.*, 2013]. The concept and structure are the same for the two model code versions.

Within a three-dimensional model domain, a geometric structure of cells is defined. Each cell is labeled with a material of a certain chemical composition (given in atomic or weight fractions) and density. The horizontal domain is set to 400 m times 400 m. We also tested a model domain of 2000 m times 2000 m but obtained similar simulation results. In order to save computer time, the complete atmosphere is not modeled. Instead, the vertical extent of the model was set to around 2 km and a modeled energy spectrum of incoming cosmic ray neutrons at 2 km is used [Hughes and Marsden, 1966]. The particle source is located at the center of the upper boundary and the released particles are a distribution of high-energy particles representative of the spectrum of incoming cosmic rays traveling through the atmosphere. A dry air by volume composed of 79% nitrogen and 21% oxygen is modeled. In order to model neutron intensities at the measured heights, a vertical discretization of 1 m is used between 0 and 28 m elevation. For higher elevations, a coarser vertical discretization is used. The neutron intensity detectors specified in the model are 1 m high layers extending the full horizontal model domain. The modeled cosmic ray neutron intensities are relative and are expressed as neutron fluence, i.e., the number of neutrons crossing a unit area (neutrons/cm²). The neutron fluences are normalized per unit source particle by the model [Zweck et al., 2013]. The number of particles released at the top of the atmosphere is balanced to obtain acceptable levels of uncertainty and manageable computational running times. For each run, we simulate at least 3 million particle histories. The model domain is constrained by reflecting surfaces, i.e., particles hitting the model boundaries will be reflected specularly back into the model domain.

Two model conceptualizations are used. First, reference models with 4 m of water of varying chemical composition are considered corresponding to brackish water, freshwater, and saltwater. For the former, the measured chemical composition at Ringkøbing Fjord is used while standard values are used for the two

latter water types (see Table 1). Second, the terrestrial environment at the Voulund Farmland on 23 September 2015 is modeled. Both a simple and a more complex model setup are applied. The prior is modeled using the MCNPX model code, while the latter is modeled with both code versions. The soil of the simple model consists of pure SiO₂. The more complex model incorporates the measured chemical composition, the organic carbon content of the soil, and the assumed Gd concentration (see Table 1). Since the fields were harvested in August 2015, bare ground conditions are used in the modeling.

The energy response of the neutron detectors may also be modeled by including the detector geometry and materials (chemical composition and density) as part of the model [e.g., Clem and Dorman, 2000]. In this case, the modeled and measured responses are directly comparable. Modeling the detector would nonetheless result in a substantial increase in the computational demand as the uncertainty of the modeled results is related to the size of the detector. This study is considered to be a first step toward increasing the understanding of the detector response and enable modeling of measured neutron intensities; yet future studies should naturally consider applying the modeling approach as well.

3.6. Measured and Modeled Neutron Energies

The modeled thermal and fast neutron intensity energy ranges are schematically depicted in Figures 3g and 3h, respectively. The measured and modeled neutron intensities are not identical even when the cadmium difference method is used. The energy ranges of the measured and modeled thermal intensities are in principle the same. However, the exact sensitivity of the bare detector to neutrons of varying thermal energies is not fully understood. This is illustrated by the smaller red area in Figure 3e compared to the red area in Figure 3g. The energy range of the moderated detector covers the entire epithermal energy range (>0.5 eV) and not only the fast neutron range (10–1000 eV). Furthermore, the exact sensitivity of the detector to the varying energy ranges is again unknown, but is expected to decrease away from fast neutron energy range. This mismatch is illustrated by the different ranges and vertical extent of the blue area in Figures 3d and 3h. The intravariability of the behavior and transport of neutrons is low within the final energy ranges (<0.5 eV for thermal and >0.5 eV for epithermal neutrons), while the intervariability between the thermal and epithermal energy ranges are significantly different [Desilets et al., 2009]. For that reason, although the energy ranges and sensitivities of measured and modeled thermal and epithermal neutron intensities are not completely identical, they are still comparable.

4. Results

4.1. Cadmium Difference Method

The results of the cadmium difference method for Gludsted Plantation and Ringkøbing Fjord are presented in Figures 4 and 5. The results of the Wüstebach Test Site are similar to the Gludsted Plantation, and are not presented.

The same trends are observed for the different sites (Figures 4 and 5). First and most apparent is the high thermal contribution to the moderated detector, especially at the ground surface. It amounts to approximately 45% of the thermal neutron intensity measured by the bare detector. The high density of elements in the ground compared to the air results in a proportional larger production of thermal neutrons in the soil. Thermal neutrons travel a relative short distance before being absorbed. For that reason, a distinctly higher concentration of thermal neutrons, and therefore also thermal contribution to the moderated detector, is recorded at the ground surface in relation to the canopy surface. Second, the epithermal contribution of the bare detector is less pronounced (between 4 and 5%) and only appears to vary slightly with height.

4.2. Neutron Energy Correction Factors

The thermal contribution to the moderated detector as a function of the thermal neutron intensities measured by the bare detector for the Gludsted Plantation and the Wüstebach Test Site are shown in Figures 6a and 6b, respectively. In Figures 7a and 7b, we similarly present the epithermal contribution of the bare detector as a function of the epithermal neutron intensities measured by the moderated detector for the Gludsted Plantation and the Wüstebach Test Site, respectively.

Linear regression models are found to adequately describe the relationships of the Gludsted Plantation presented in Figures 6 and 7 (see Table 2 for obtained model parameters). At the Wüstebach Test Site, we only have measurements at the ground and the canopy surface thus leading to a plot of only two clusters. We recognize that a linear model fit to a two-clustered data set is inappropriate. However, based on the fact

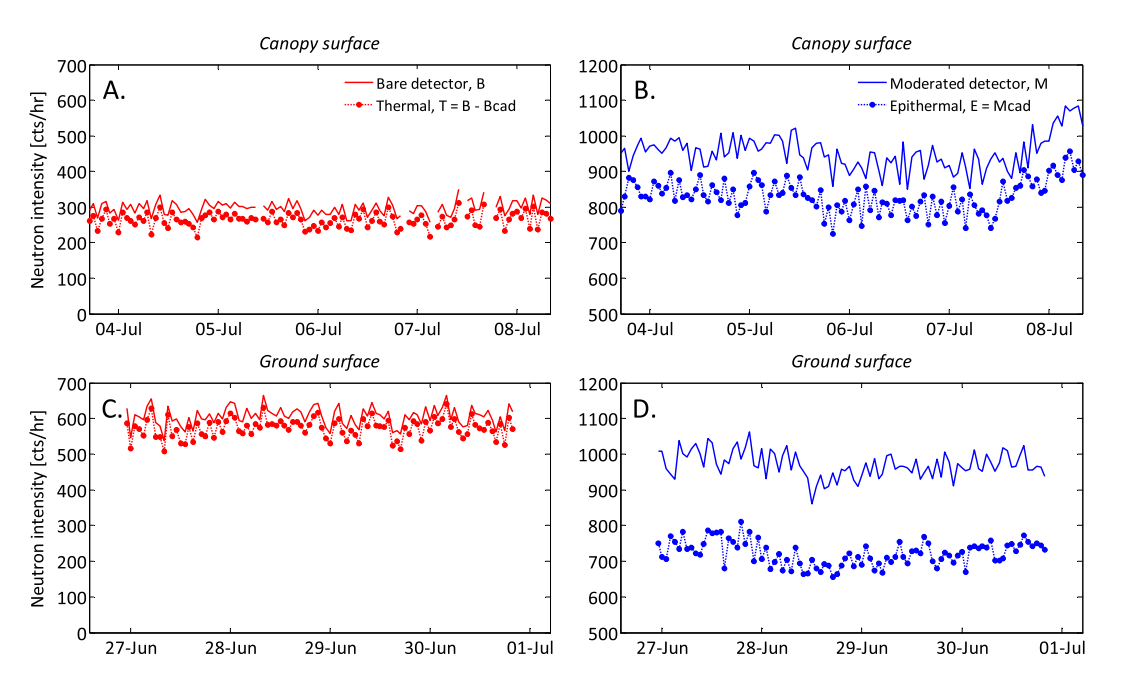


Figure 4. Neutron intensities (hourly data) obtained from field campaigns conducted at the Gludsted Plantation. (a) Neutron intensity measured by the bare detector (Figure 3a) and the computed thermal neutron intensity (Figure 3e) using the cadmium difference method at the canopy surface on 3–8 July 2014. (b) Neutron intensity measured by the moderated detector (Figure 3b) and the cadmium-shielded moderated detector (Figure 3d) at the canopy surface on 3–8 July 2014. (c) The neutron intensity measured by the bare detector (Figure 3a) and the computed thermal neutron intensity (configuration as in Figure 3e) at the ground surface on 26–30 June 2014. (d) Neutron intensity measured by the moderated detector (Figure 3b) and the cadmium-shielded moderated detector (Figure 3d) at the ground surface on 26–30 June 2014.

that linear relationships can be obtained for the Gludsted Plantation, we assume this also to be valid for the Wüstebach Test Site. The relationship describing the measurements at the Wüstebach Test Site is only used to accentuate the difference between the two field sites. At the Gludsted Plantation/Ringkøbing Fjord, the data are also clustered, nonetheless, the measurements of the clusters spread more and represent a considerable range of values, justifying the linear model fit. The coefficient of determination (R^2) at the Gludsted Plantation/Ringkøbing Fjord and the Wüstebach Test Site is 0.964 and 0.984 for the thermal neutron intensity model (Figure 6), and 0.637 and 0.870 for the epithermal neutron intensity model (Figure 7), respectively. The variance of the residuals of the thermal and epithermal neutron models are similar. However, the total variance of the epithermal neutron intensity model is small resulting in lower R^2 values. Uncertainty on the measured neutron intensities are indicated using ± 1 standard deviation for a low and a high neutron intensity measurement point.

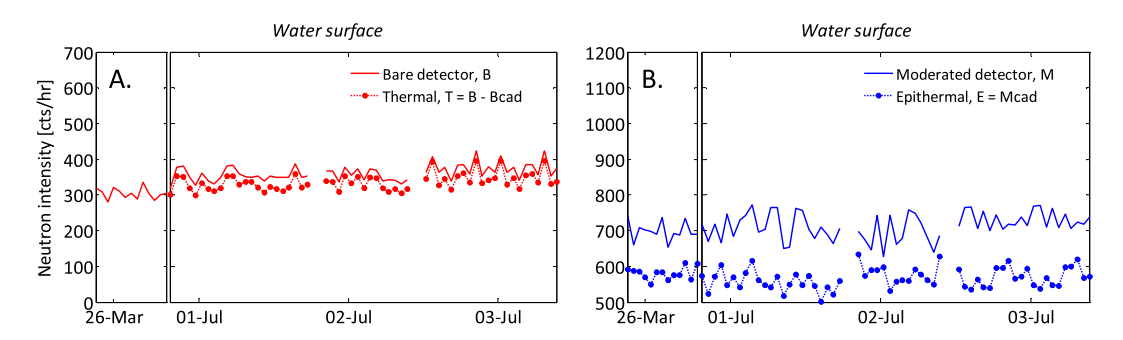


Figure 5. Neutron intensities (hourly data) obtained from field campaigns conducted at the Ringkøbing Fjord at 0.5 m height above the water surface during 25–26 March 2014 and 30 June 2014 to 3 July 2014. The cadmium difference method was performed for the moderated detector during the first campaign and for both the bare and the moderated detector during the second campaign. (a) Neutron intensity measured by the bare detector (Figure 3a) and computed thermal neutron intensity using the cadmium difference method (Figure 3e). (b) Neutron intensity measured by the moderated detector (Figure 3b) and the cadmium-shielded moderated detector (Figure 3d).

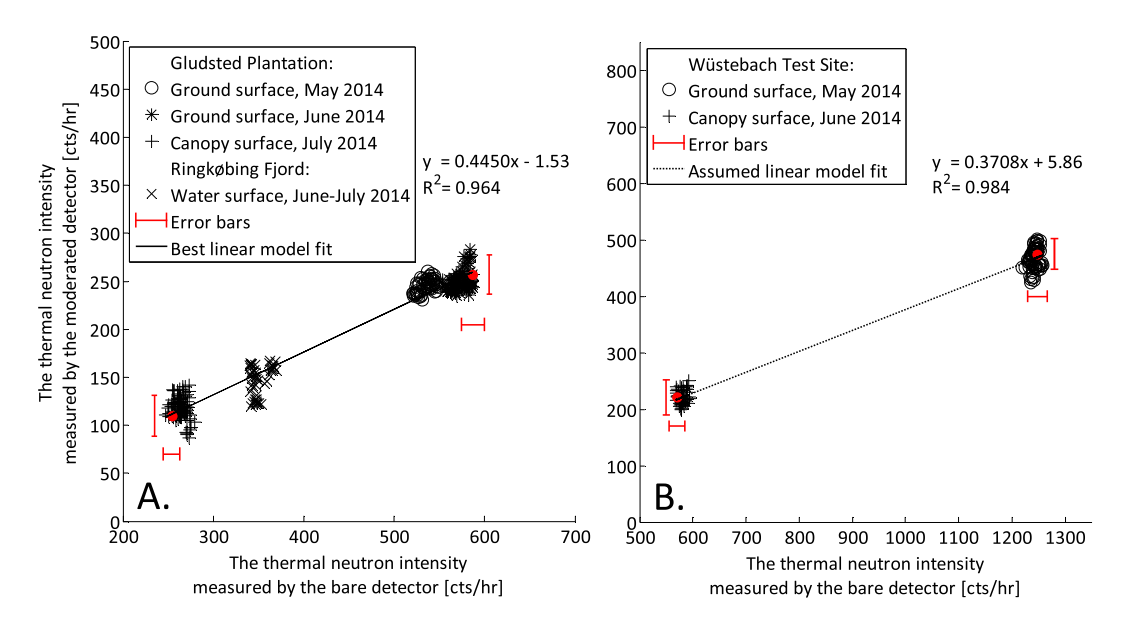


Figure 6. Scatterplot of the thermal neutron intensity measured by the bare detector (as in Figure 3e) and the thermal contribution measured by the moderated detector (as in Figure 3f) (12 h average). (a) The Gludsted Plantation (CR1000/B system). (b) The Wüstebach Test Site (CR2000/B system). Measurement error bars corresponding to ± 1 standard deviation representative for a low and a high value data point.

The observed relationships are not exactly the same at the Gludsted Plantation/Ringkøbing Fjord and at the Wüstebach Test Site. As the thicknesses of the moderators are the same for the detectors of the CR1000/B system and the CR2000/B system one would expect that the same fraction of thermal neutrons is transmitted through the plastic, resulting in a universal relationship. However, this would require that the thermal/epithermal neutron ratio should be identical regardless of the detectors used. This is unlikely due to different gas types and pressure (detailed above). At this point in time, it is unclear whether local environmental settings also affect the relationship and we recommend future studies to address this issue. However, it should be mentioned that the same relationship is obtained from the two field sites of significantly different land cover settings (the Gludsted Plantation and the Ringkøbing Fjord).

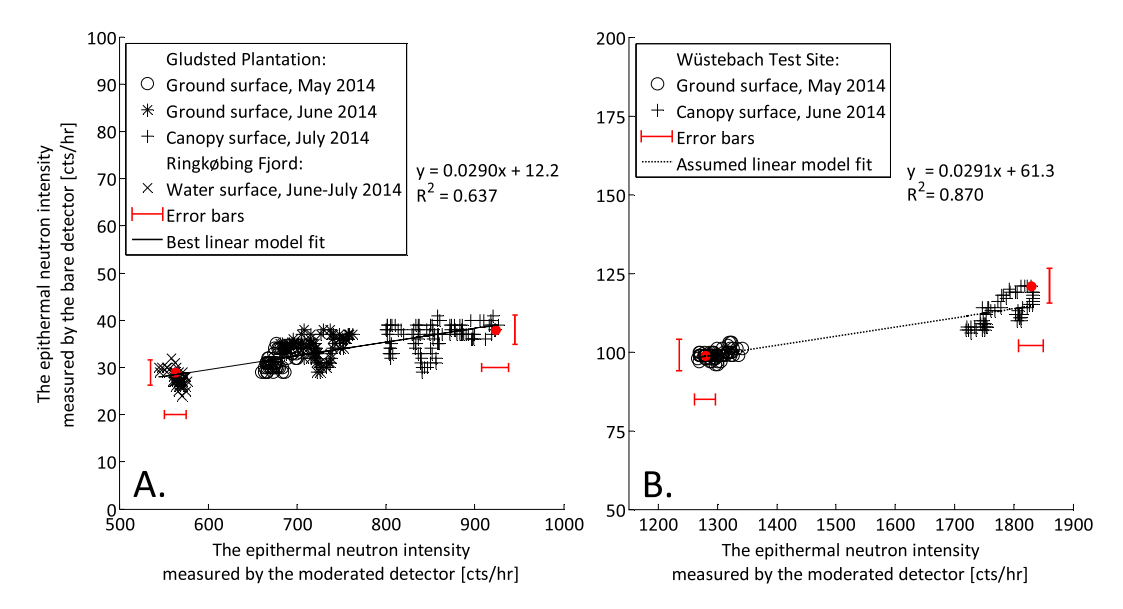


Figure 7. Scatterplot of epithermal neutrons measured by the moderated detector (as in Figure 3d) and the epithermal contribution measured by the bare detector (as in Figure 3c) (12 h moving average). (a) The Gludsted Plantation (CR1000/B system). (b) The Wüstebach Test Site (CR2000/B system). Measurement error bars corresponding to ±1 standard deviation representative for a low and a high value data point.

Table 2. Model Parameters $(\alpha_1,\alpha_2,\beta_1,$ and $\beta_2)$ for the Calculation of Thermal and Epithermal Neutron Intensities Using the CR1000/B System at the Gludsted Plantation and the Ringkøbing Fjord, and the CR2000/B System at the Wüstebach Test Site, Respectively

| | Gludsted Plantation and Ringkøbing Fjord | Wüstebach Test Site | |
|---|---|--------------------------|--|
| α_1 β_1 (cts/h) α_2 | 0.0290 12.2 0.445 | 0.0291 61.3 0.3708 | |
| β_2 (cts/h) | -1.53 | 5.862 | |

The potential difference in the footprint of the bare and the moderated neutron detector is a concern when combining measurements of the two detectors. Lateral homogeneity in soil, vegetation, and litter layer prevails at the field sites and comparability is therefore assumed even if the footprint of the bare and the moderated detector prove to be different.

Assuming that the relationships shown in Figures 6 and 7 are linear and the measurements of the bare and the moderated detection are comparable,

equations expressing the moderated (M) and the bare (B) neutron intensities as a function of thermal (T) and epithermal (E) neutron intensities can be developed, see equations (3) and (4).

$$B = T + \alpha_1 E + \beta_1 \tag{3}$$

$$M = E + \alpha_2 T + \beta_2 \tag{4}$$

The epithermal contribution is assumed to be a fraction (α_1) of the epithermal neutron intensity measured by the moderated detector and an offset (β_1) . Similarly, the thermal contribution is assumed to be a fraction (α_2) of the thermal neutron intensity measured by the bare detector and an offset (β_2) . The model parameters α and β are determined from results of the cadmium difference method (Figures 6 and 7).

The offsets β_1 and β_2 in equations (3) and (4) are included as they account for the fact that the energy ranges, are not completely in agreement, as illustrated in Figure 3. The bare detector measures the whole energy spectrum of 0–0.5 eV (Figure 3e), whereas the energy of the thermal contribution to the moderated detector is restricted to the higher end of the thermal energy range (Figure 3f) since the neutrons of lower energies are absorbed by the moderator. Contrary to this, the bare detector measures only the lower end of the epithermal energy range (Figure 3c), while the whole epithermal energy range is measured by the moderated detector (Figure 3d).

By rearranging equations (3) and (4), we obtain the following functions to compute the thermal and epithermal components from the measurements of the bare and moderated neutron detectors:

$$T = \frac{B - \beta_1 - \alpha_1 M + \alpha_1 \beta_2}{1 - \alpha_1 \alpha_2} \tag{5}$$

$$\mathsf{E} = \frac{\mathsf{M} - \beta_2 - \alpha_2 \mathsf{B} + \alpha_2 \beta_1}{1 - \alpha_1 \alpha_2} \tag{6}$$

4.3. Impact of Neutron Energy Correction Factors

The neutron intensity profiles measured at the Gludsted Plantation using the bare and moderated detectors in November 2013 and March 2014 are shown in Figures 8a and 8b, respectively. Using equations (5) and (6) as well as the determined model parameters provided in Table 2, the thermal and epithermal neutron intensity profiles are estimated (Figures 8c and 8d). Due to the minor epithermal contribution, only a small difference appears when comparing the bare and the thermal neutron intensity profile. Both profiles illustrate the considerable decreases in thermal neutron intensity with height above the ground surface in line with the expected from theory. However, the effect of correcting the moderated detector is substantial. Prior to correction, the profiles exhibit no obvious trend as a function of height. After correction, an increase with height is observed. This is in agreement with theory [Desilets et al., 2009, Figure 2] and the measured epithermal profile in March 2014 (Figure 8d).

Uncorrected and corrected continuous time series measurements at the Gludsted Plantation (2013–2015) are shown in Figure 9. Before correction, ground surface neutron intensities measured by the moderated detector are similar or higher (e.g., year 2013 in Figure 9a) than the neutron intensities measured at canopy

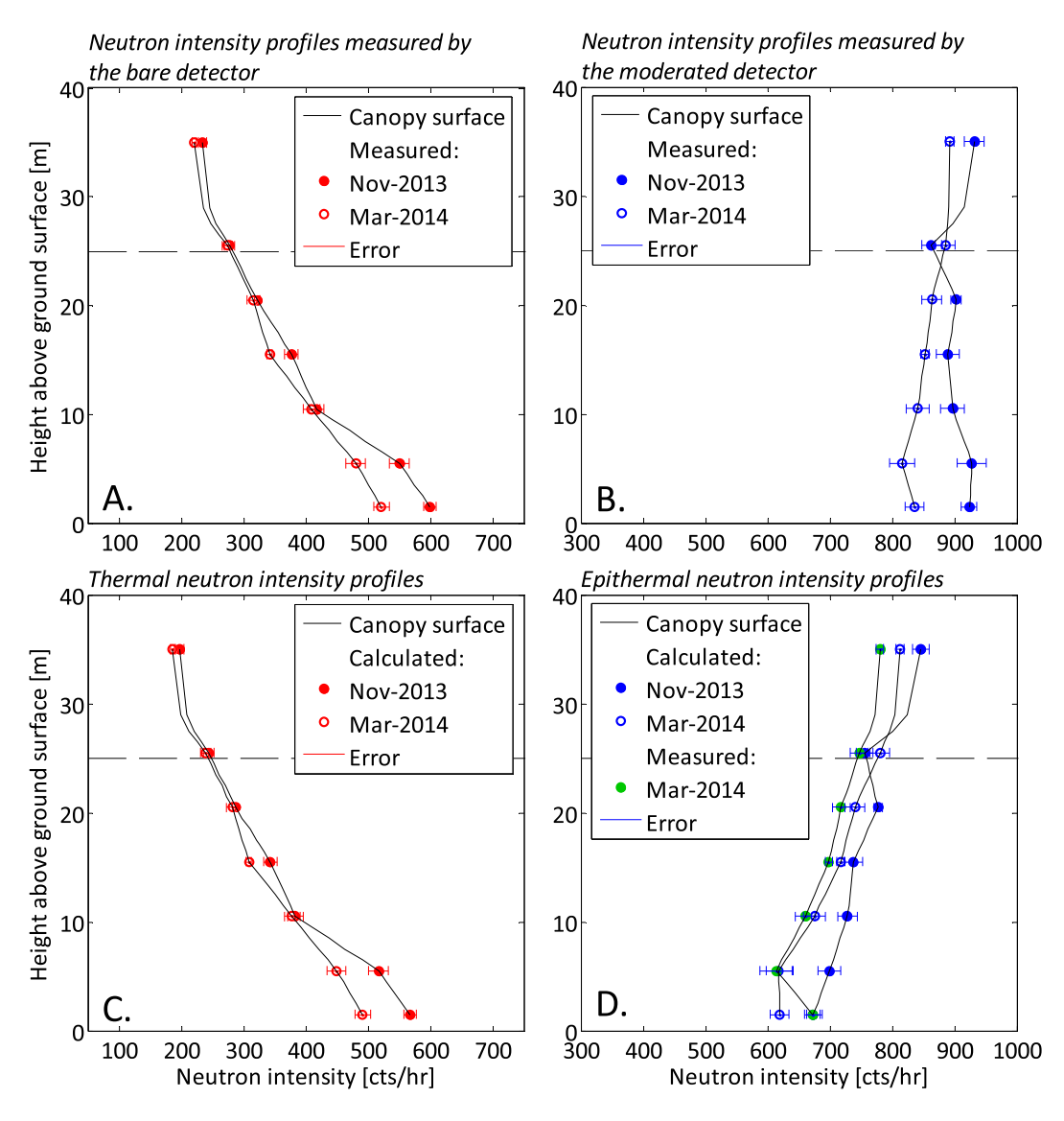


Figure 8. Neutron profiles from the ground surface to 35 m height at the Gludsted Plantation in November 2013 and March 2014. (a) Neutron profiles measured by the bare detector. (b) Neutron profiles measured by the moderated detector. (c) Thermal neutron intensity profiles estimated using the neutron energy correction model. (d) Epithermal neutron intensity profiles measured (March 2014) and estimated (November 2013 and March 2014) using cadmium-shielded moderated detector and the neutron energy correction model, respectively.

surface. Higher neutron intensities at ground level would only be present at extreme dry conditions [Desilets et al., 2009] (unlikely to be found in Denmark). After correction, the epithermal neutron intensities at ground level are significantly lower than at canopy level for the entire 2 year period (Figure 9b) and is a result of the much larger thermal neutron contribution to the moderated detector at the ground surface compared to the canopy surface.

As demonstrated, removing the epithermal and thermal contribution has a significant effect on the detected profiles. This effect is of great importance when using epithermal neutron intensities from more than one height or when comparing measured and modeled neutron intensities.

4.4. Model-To-Measurements Conversion Factors

Model-to-measurements conversion factors are estimated in order to be able to compare measured and modeled neutron intensity values. These are obtained by comparing measurements at reference conditions (above a large water body) with modeling results for similar conditions. A water body is chosen as reference

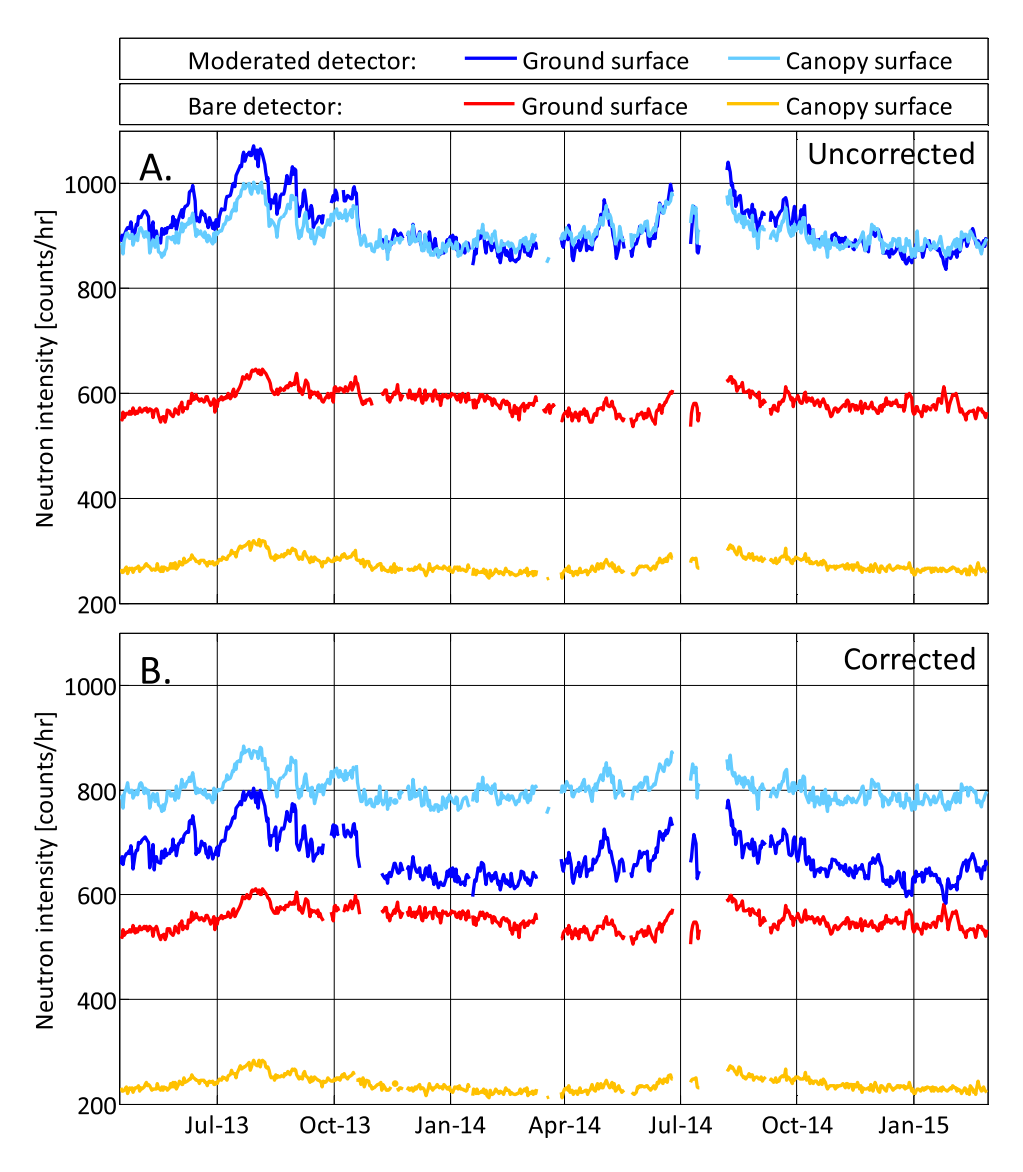


Figure 9. Neutron intensity at the Gludsted Plantation in the period April 2013 to March 2015 (daily moving average). (a) Neutron intensity measured by the bare and the moderated detector at the ground and canopy surface. (b) Estimated thermal and epithermal neutron intensity at the ground and canopy surface using the neutron energy correction equations and the neutron intensity measured by the bare and moderated detector.

as it is much less complex and less heterogeneous than a terrestrial field site and thus can more accurately be modeled using a simple model setup.

From the reference neutron intensities measured at the Ringkøbing Fjord in March and July 2014 (Figure 5), some noticeable changes are visible. Although fluctuating, no significant change over time appears to exist in the neutron intensity measured by the moderated detector. Contrary to this, neutron intensities measured by the bare detector change over time corresponding to an approximately 25% increase in the intensity. The changes in intensities could be related to the temporal variations in salinity at the Ringkøbing Fjord.

Neutron intensity profile results from three setups of varying salinity and water density modeled using the MCNPX model are presented in Figure 10 (see Table 1 for details of water properties). One of these three models represents the measured reference condition at the Ringkøbing Fjord on 30 June 2014.

The model results confirm the importance of salinity on thermal neutron intensities. The chloride concentration is the main contributor to the changes in the thermal neutron intensity. Chloride has a high neutron

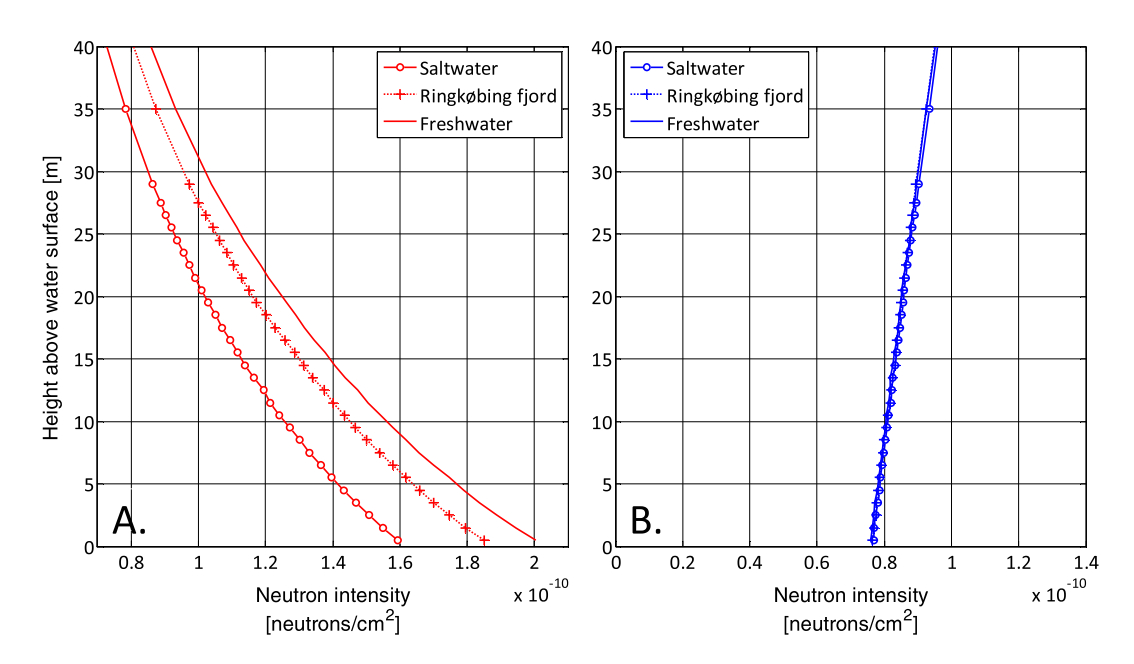


Figure 10. Modeled neutron intensity profiles above saltwater, freshwater, and water with the chemical composition measured at the Ringkøbing Fjord 30 June 2014 using the MCNPX model code. (a) Thermal neutron intensity profiles. (b) Fast neutron intensity profiles.

absorption cross section (33.5 barn) [Sears, 1992]. As a result, an inverse relation is found between chloride and the neutron intensity, similar to hydrogen.

Based on the modeled relative thermal and fast neutron intensities obtained from the MCNPX model code (shown in Figure 10) and the MCNP6 model code (not presented), as well as measured values of thermal and epithermal neutron intensities from 30 June 2014 (Figure 5) model-to-measurements conversion factors are determined. The thermal and epithermal neutron intensity model-to-measurements conversion factors are 1.705 \times 10¹² and 7.174 \times 10¹² for the MCNPX model code, respectively, and 3.739 \times 10¹² and 1.601 \times 10¹³ for the MCNP6 model code, respectively. These values are multiplied with the modeled thermal and fast neutron fluences and we emphasize that these conversion factors are detector specific.

4.5. Method Verification

The proposed methodology for comparing modeled and measured neutron intensities is tested for the Voulund Farmland agricultural field site using the available site-specific measurements. In a subsequent contribution, we also test the methodology for the Gludsted Plantation, which is much more complex and computationally more demanding than the agricultural site.

Using equations (5) and (6) as well as the model parameters provided in Table 2, thermal and epithermal neutron intensity profiles are estimated at the Voulund Farmland (Figure 11). The modeled thermal and fast neutron intensities of a simple and a more complex model-setup for the Voulund Farmland are converted using the model-to-measurements conversion factors obtained for the specific detector system and model code.

The gradient of the modeled thermal and fast neutron intensity profiles are for both the simple and complex model-setups in very good agreement with the measured profiles. An average difference of 66 and 202 counts/h between measured and modeled thermal and epithermal/fast neutron intensities, respectively, are obtained for the simple model-setup for the Voulund Farmland (pure SiO₂). This setup has previously been used when modeling neutron intensity [Desilets et al., 2010; Franz et al., 2012b]. As anticipated using site-specific characteristics in the model-setup, lead to a better agreement of measured and modeled neutron intensities. The average differences between measured and modeled thermal and epithermal/fast neutron intensity then using the MCNPX model code are reduced to 15 and 131 counts/h, respectively. The MCNP6 model code results in a higher average difference in measured and modeled thermal neutron intensities (53 counts/h) relative to the complex model-setup modeled using the MCNPX model code. Despite

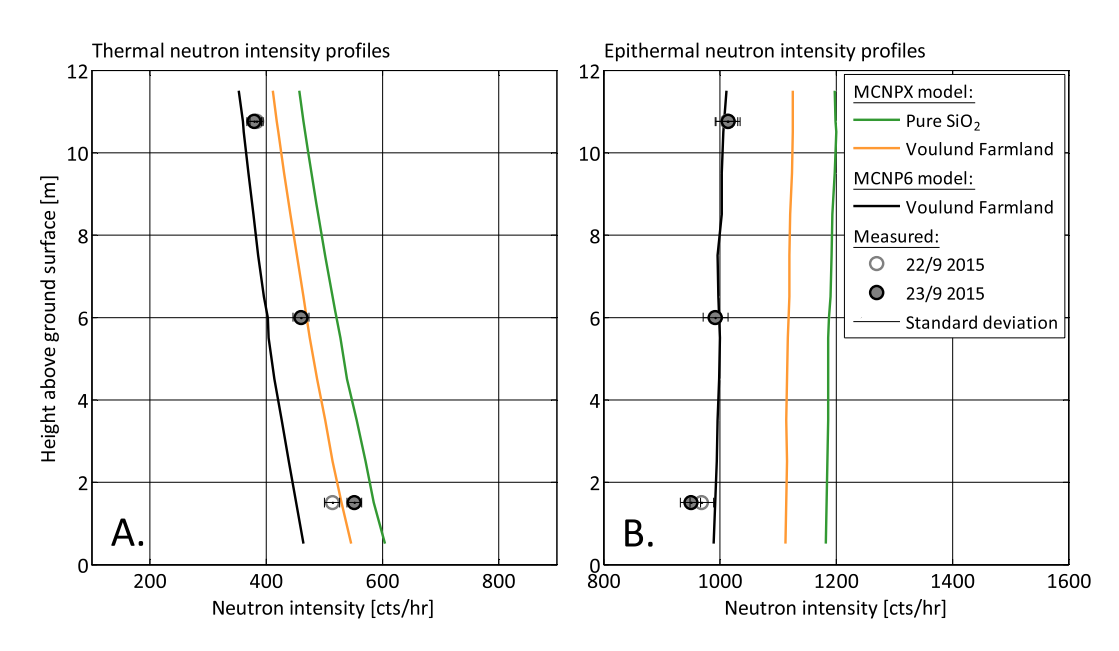


Figure 11. Neutron intensity profiles at the Voulund Farmland on 22 and 23 September 2015. A simple model-setup of pure SiO₂ soil is modeled using the MCNPX model code and a more complex model-setup including the measured soil chemical composition and soil organic carbon is modeled using both the MCNPX and the MCNP6 model code. The measured thermal and epithermal neutron intensity profiles are obtained using the neutron energy correction models for the neutron intensities measured by the bare and moderating detectors. (a) Measured and modeled thermal neutron intensities. (b) Measured epithermal neutron intensities and modeled fast neutron intensities

this, the MCNP6 model code is assessed to perform better overall as the fit of measured and modeled epithermal/fast neutron intensities has improved considerably (with an average difference in measured and modeled epithermal/fast neutron intensity of 11 counts/h).

We consider these differences to be satisfactory, especially as many factors may contribute to discrepancies between measurements and modeling.

The measurements are subject to several uncertainties including:

- 1. The determination of the model-to-measurements conversion factors was based on measurements from only one field campaign and one height level.
- 2. The footprint of the bare and the moderated detector are unexplained and ambiguous, respectively. This is explained in section 3.2.
- 3. Measured neutron intensities at the Danish field sites were relatively low because they were close to sea level.
- 4. The effect of atmospheric water vapor on the thermal neutron intensity at various heights is not well understood.
- 5. The correction for variations in incoming cosmic ray intensity is based on observations from Switzerland at lower latitude and higher altitude.

In addition, several modeling uncertainties are introduced:

- 1. A general energy spectrum of incoming cosmic ray particles is used and its possible spatial and temporal variations could be of importance.
- 2. Homogeneous soil/water and land cover conditions are assumed.
- 3. The water chemistry used for neutron transport modeling at the Ringkøbing Fjord was determined from only a single water sample collected on the day of neutron detection.
- 4. An incomplete chemical analysis of the soil.

These issues need to be further analyzed in future studies.

We found thermal and fast neutrons to be sensitive to soil chemistry, and we therefore suggest the effect of other environment variables and parameters (e.g., vegetation, intercepted precipitation, and rare earth element) on thermal and fast neutron intensities to be quantified through a more thorough sensitivity analysis. Such an analysis would improve the basis for modeling and may result in better agreement between measured and modeled neutron intensity profiles.

We recommend the proposed methodology to be applied for studies combining neutron detection and modeling to ensure comparability. This is especially true then multiple height levels are considered as the magnitude of the epithermal and thermal neutron contribution to the bare and the moderated detector, respectively, changes with height. The measured neutron intensity is reduced using cadmium-shielded neutron detectors and therefore results in increased uncertainties (following the Poissonian statistics). However, removal of the epithermal and thermal neutron contribution to the bare and moderated detector, respectively, provide neutron signals of well-defined neutron energy ranges. Thus, the uncertainty related to lumping neutrons of different physical behaviors is reduced.

5. Conclusion

In this study, a methodology was developed to improve the comparison between measured and modeled thermal and epithermal neutron intensities above the land surface.

First, neutron energy correction models used to estimate thermal and epithermal intensities were developed. The models were found to adequately describe the relationships at Gludsted Plantation/Ringkøbing Fjord, while the data set at Wüstebach Test Site was found to be insufficient. Nonetheless, based on the findings at the Danish field sites, linear relationships were also assumed at Wüstebach Test Site. However, the use of another cosmic ray neutron system and the different environmental settings may significantly change the relationship. In order to validate the assumed linear relationships of the bare and the moderated detectors at Wüstebach Test Site, a more extensive data set is therefore required. Contrary to modeled neutron intensities of energies 0–0.5 eV (thermal neutrons) and 10–1000 eV (fast neutrons), measured energy ranges are less well defined. The energy range, distribution, and the sensitivity to the distribution of neutrons of different energies within the range are not well understood. The cadmium difference method was used to distinguish the contribution of epithermal and thermal neutrons to the intensity measured by the bare and moderated detectors at three different field sites, respectively. The fraction of epithermal neutrons contributing to the neutron intensity measured by the bare detector was found to be relatively small, but the moderated detector was subject to a larger fraction of thermal neutrons. The contribution of epithermal and thermal neutrons to the intensities measured by the bare and moderated detectors, respectively, were found to be independent of the measurement height.

Based on the results of the cadmium difference method, neutron energy correction models were derived enabling thermal neutron intensities to be determined by the bare detector, and epithermal neutron intensities to be determined by the moderated detector. The models were found to be nonuniversal and must be developed for the specific detector systems in use. Thus, two different neutron energy correction models were derived in this study; one for the detector system of the Gludsted Plantation and the Ringkøbing Fjord, and another for the detector system of the Wüstebach Test Site. The difference of the two neutron energy correction models is caused by different thermal-to-epithermal neutron ratios, however, there may also be a component of unknown magnitude related to environmental settings.

Second, model-to-measurements conversion factors were computed to enhance the comparability between measured and modeled neutron intensity. They were determined by relating the modeled neutron intensity to the measured neutron intensity above a water body. The factors were computed for a water body as the settings here are less complex and simpler to model as compared to a terrestrial field site. For thermal and epithermal/fast neutron intensities at the Gludsted Plantation and the Ringkøbing Fjord, the model-to-measurements conversion factors were determined to be 1.705×10^{12} and 7.174×10^{12} for the MCNPX model code and 3.739×10^{12} and 1.601×10^{13} for the MCNP6 model code, respectively.

Third, we verified our methodology using data from the Voulund Farmland agricultural field site. Two model setups were tested using the MCNPX model code: a simple and commonly used model assuming soil material composed of pure SiO₂ and a more complex model based on site-specific data including soil chemistry and soil organic carbon. The latter model provided neutron intensities which were in acceptable agreement with measurements, yet differences between measured epithermal neutrons and modeled fast neutrons were still significant. The results of the more complex model-setup, using the

newer and more advanced MCNP6 model code version, slightly underestimated thermal neutrons, while satisfactory agreement of measured epithermal and modeled fast neutron intensity profiles were obtained. The remaining discrepancy is due to a number of uncertainty factors related to both measurement and modeling techniques. Nevertheless, application of the method is recommended for studies combining neutron detection and modeling, especially then multiple height levels are considered. Neutron transport modeling of both thermal and epithermal neutrons is a valuable tool examining the prospects of further development of the soil moisture estimation method and the potential of additional applications. For site-specific modeling, it is important to include an adequate description of the soil matrix including soil chemistry, soil moisture and bulk density. We anticipate that the proposed methodology offers promising perspectives in the use of the cosmic ray neutron technique, e.g., developing methods to separate the signals of the different pools of hydrogen and thus is of great relevance for hydrological purposes.

Acknowledgments

The Villum Foundation (www. villumfonden.dk) is greatly thanked for funding the HOBE project (www.hobe. dk). Special thank goes to Lars Rasmussen and Anton G. Thomsen (Aarhus University) for the extensive help in the field. We acknowledge the NMDB database (www.nmdb.eu), founded under the European Union's FP7 programme (contract 213007) for providing data. Jungfraujoch neutron monitor data were kindly provided by the Cosmic Ray Group, Physikalisches Institut, University of Bern, Switzerland. Data used for this study are available from the lead author (mie.andreasen@ ign.ku.dk).

References

- Appelo, C. A. J., and D. Postma (2005), *Geomchemistry, Groundwater and Pollution*, 2nd ed., 649 pp., Balkema, Rotterdam, Amsterdam, Netherlands
- Baatz, R., H. R. Bogena, H.-J. Hendricks Franssen, J. A. Huisman, W. Qu, C. Montzka, and H. Vereecken (2014), Calibration of a catchment scale cosmic-ray probe network: A comparison of three parameterization methods, *J. Hydrol.*, *516*, 231–244, doi:10.1016/i.jhydrol.2014.02.026.
- Baatz, R., H. R. Bogena, H.-J. Hendricks Franssen, J. A. Huisman, C. Montzka, and H. Vereecken (2015), An empirical vegetation correction for soil moisture content quantification using cosmic ray probes, *Water Resour. Res.*, 51, 2030–2046, doi:10.1002/2014WR016443.
- Bethe, H. A., S. A. Korff, and G. Placzek (1940), On the interpretation of neutron measurements in cosmic radiation, *Phys. Rev.*, 57, 573–587, doi:10.1103/PhysRev.57.573.
- Bogena, H. R., J. A. Huisman, R. Baatz, H.-J. Hendricks-Franssen, and H. Vereecken (2013), Accuracy of the cosmic-ray soil water content probe in humid forest ecosystems: The worst case scenario, Water Resour. Res., 49, 5778–5791, doi:10.1002/wrcr.20463.
- Bogena, H. R., et al. (2015), A terrestrial observatory approach for the integrated investigation of the effects of deforestation on water, energy, and matter fluxes, Sci. China Earth Sci., 58(1), 61–75, doi:10.1007/s11430-014-4911-7.
- Clem, J. M., and L. I. Dorman (2000), Neutron monitor response functions, *Space Sci. Rev.*, 93, 335–359, doi:10.1023/A:1026508915269. Chrisman, B., and M. Zreda (2013), Quantifying mesoscale soil moisture with the cosmic-ray rover, *Hydrol. Earth Syst. Science*, 17, 5097–5108. doi:10.5194/hess-17-5097-2013.
- Desilets, D., and M. Zreda (2001), On scaling cosmogenic nuclide production rates for altitude and latitude using cosmic-ray measurements, *Earth Planet. Sci. Lett.*, 193, 213–225, doi:10.1016/S0012-821X(01)00477-0.
- Desilets, D., and M. Zreda (2003), Spatial and temporal distribution of secondary cosmic-ray nucleon intensities and applications to in situ cosmogenic dating, *Earth Planet. Sci. Lett.*, 206, 21–42, doi:10.1016/S0012-821X(02)01088-9.
- Desilets, D., and M. Zreda (2013), Footprint diameter for a cosmic-ray soil moisture probe: Theory and Monte Carlo simulations, *Water Resour. Res.*, 49, 3566–3575, doi:10.1002/wrcr.20187.
- Desilets, D., M. Zreda, and T. Prabu (2006), Extended scaling factors for in situ cosmogenic nuclides: New measurements at low latitude, *Earth Planet. Sci. Lett.*, 246, 265–276, doi:10.1016/j.epsl.2006.03.051.
- Desilets, D., N. Mascarenhas, P. Marleau, and J. S. Brennan (2009), Land-surface hydrology with a directional neutron detector, *Rep. SAND2009-6321*, Sandia Natl. Lab, Albuquerque, New Mexico 87185 and Livermore, Calif.
- Desilets, D., M. Zreda, and T. P. A. Ferré (2010), Naturés neutron probe: Land surface hydrology at an elusive scale with cosmic rays, *Water Resour. Res.*, 46, W11505, doi:10.1029/2009WR008726.
- Dong, J., T. E. Ochsner, M. Zreda, M. H. Cosh, and C. B. Zou (2014), Calibration and validation of the COSMOS rover for surface soil moisture measurement, *Vadose Zone J.*, 13(4), doi:10.2136/vzj2013.08.0148.
- Dunkerley, D. (2000), Measuring interception loss and canopy storage in dryland vegetation: A brief review and evaluation of available research strategies, *Hydrol. Processes*, 14(4), 669–678, doi:10.1002/(SICI)1099-1085(200003)14:43.0.CO;2-I.
- Franz, T. E., M. Zreda, R. Rosolem, and T. P. A. Ferre (2012a), Field validation of a cosmic-ray neutron sensor using a distributed sensor network, *Vadose Zone J.*, 11(4), doi:10.2136/vzj2012.0046.
- Franz, T. E., M. Zreda, T. P. A. Ferre, R. Rosolem, C. Zweck, S. Stillman, X. Zeng, and W. J. Shuttleworth (2012b), Measurement depth of the cosmic ray soil moisture probe affected by hydrogen from various sources, *Water Resour. Res.*, 48, W08515, doi:10.1029/2012WR011871.
- Franz, T., M. Zreda, R. Rosolem, B. K. Hornbuckle, S. Irvin, H. Adams, T. E. Kolb, C. Zweck, and W. J. Shuttleworth (2013a), Ecosystem-scale measurements of biomass water using cosmic-ray neutrons, *Geophys. Res. Lett.*, 40, 3929–3933, doi:10.1002/grl.50791.
- Franz, T., M. Zreda, R. Rosolem, and T. P. A. Ferre (2013b), A universal calibration function for determination of soil moisture with cosmic-ray neutrons, *Hydrol. Earth Syst. Sci.*, 17(2), 453–460, doi:10.5194/hess-17-453-2013.
- Franz, T. E., T. Wang, W. Avery, C. Finkenbiner, and L. Brocca (2015), Combined analysis of soil moisture measurements from roving and fixed cosmic ray neutron probes for multiscale real-time monitoring, *Geophys. Res. Lett.*, 42, 3389–3396, doi:10.1002/2015GL063963.
- Glasstone, S. and M. C. Edlund (1952), The Elements of Nuclear Reactor Theory, 5th ed., 416 pp., Van Nostrand, N. Y.
 Goldhagen, P., M. Reginatto, T. Kniss, J. W. Wilson, R. C. Singleterry, I. W. Jones, and W. Van Steveninck (2002), Measurement of the energy spectrum of cosmic-ray induced neutrons aboard an ER-2 high-altitude airplane, Nucl. Instrum. Methods Phys. Res. A, 476(1), 42–51, doi: 10.1016/S0168-9002(01)01386-9.
- Goorley, J. T., et al. (2013), MCNP6TM users manual, version 1.0, *Rep. LA-CP-13-00634*, Los Alamos Natl. Lab., Los Alamos, N. M. Gordon, M. S., P. Goldhagen, K. P. Rodbell, T. H. Zabel, H. H. K. Tang, J. M. Clem, and P. Bailey (2004), Measurement of the flux and energy spectrum of cosmic-ray induced neutrons on the ground, *IEEE Trans. Nucl. Sci.*, *51*(6), 3427–3434, doi:10.1109/TNS.2004.839134.
- Haider, K., P. Engesgaard, T. O. Sonnenborg, and C. Kirkegaard (2015), Numerical modeling of salinity distribution and submarine ground-water discharge to a coastal lagoon in Denmark based on airborne electromagnetic data, Hydrogeol. J., 23, 217–233, doi:10.1007/s10040-014-1195-0.

- Hawdon, A., D. McJannet, and J. Wallace (2014), Calibration and correction procedures for cosmic-ray neutron soil moisture probes located across Australia, *Water Resour. Res.*, 50, 5029–5043, doi:10.1002/2013WR015138.
- Heidbüchel, I., A. Güntner, and T. Blume (2015), Use of cosmic ray neutron sensors for soil moisture monitoring in forests, *Hydrol. Earth Syst. Sci. Discuss.*, 12, 9813–9864, doi:10.5194/hessd-12-9813-2015.
- Hughes, E. B., and P. L. Marsden (1966), Response of a standard IGY neutron monitor, *J. Geophys. Res.*, 71(5), 1435–1444, doi:10.1029/JZ071i005p01435.
- Jenkins, J. C., D. C. Chojnacky, L. S. Heath, and R. A. Birdsey (2003), National-scale biomass estimators for United States tree species, *For. Sci.*, 49(1), 12–35.
- Jensen, K. H., and T. H. Illangasekare (2011), HOBE—A hydrological observatory in Denmark, *Vadose Zone J.*, 10, 1–7, doi:10.2136/vzj2011.0006.
- Kinnear, J. A., A. Binley, C. Duque, and P. K. Engesgaard (2013), Using geophysics to map areas of potential groundwater discharge into Ringkøbing Fjord, Denmark, *Leading Edge*, 32(7), 792–796, doi:10.1190/tle32070792.1.
- Knoll, G. F. (2010), Radiation Detection and Measurement, 3rd ed., John Wiley, Hoboken, N. J.
- Köhli, M., M. Schrön, M. Zreda, U. Schmidt, P. Dietrich, and S. Zacharias (2015), Footprint characteristics revised for field-scale soil moisture monitoring with cosmic-ray neutrons, *Water Resour. Res.*, 51(7), 5772–5790, doi:10.1002/2015WR017169.
- Lockwood, J. A., and H. E. Yingst (1956), Correlation of meteorological parameters with cosmic-ray neutron intensities, Phys. Rev., 104, 1718–1722, doi:10.1103/PhysRev.104.1718.
- McJannet, D., T. Franz, A. Hawdon, D. Boadle, B. Baker, A. Almeida, R. Silberstein, T. Lambert, and D. Desilets (2014), Field testing of the universal calibration function for determination of soil moisture with cosmic-ray neutrons, *Water Resour. Res.*, 50,5235–5248, doi:10.1002/2014WR015513.
- Nord-Larsen, T., and J. Schumacher (2012), Estimation of forest resources from a country wide laser scanning survey and national forest inventory data, *Remote Sens. Environ.*, 119, 148–157, doi:10.1016/j.rse.2011.12.022.
- Ochsner, T. E., et al. (2013), State of the art in large-scale soil moisture monitoring, Soil Sci. Soc. Am. J., 77(6), 1888–1919, doi:10.2136/sssaj2013.03.0093.
- Pelowitz, D. B. (2011), MCNPX[™] user's manual, version2.7.0, *Rep. LA-CP-11-00438*, Los Alamos Natl. Lab., Los Alamos, N. M.
- Ringgaard, R., M. Herbst, and T. Friborg (2014), Partitioning forest evapotranspiration: Interception evaporation and the impact of canopy structure, local and regional advection, J. Hydrol., 517(2014), 677–690, doi:10.1016/j.jhydrol.2014.06.007.
- Rivera Villarreyes, C. A., G. Baroni, and S. E. Oswald (2013), Calibration approaches of cosmic-ray neutron sensing for soil moisture measurement in cropped fields, *Hydrol. Earth Syst. Sci. Discuss.*, 10, 4237–4274, doi:10.5194/hessd-10-4237-2013.
- Rosolem, R., W. J. Shuttleworth, M. Zreda, T. E. Franz, X. Zeng, and S. A. Kurc (2013), The effect of atmospheric water vapor on neutron count in the cosmic-ray soil moisture observing system, *J. Hydrometeorol.*, doi:10.1175/JHM-D-12-0120.1.
- Rühm, W., V. Mares, C. Pioch, E. Weitzenegger, R. Vockenroth, and H. G. Paretzke (2009), Measurements of secondary neutrons from cosmic radiation with a Bonner sphere spectrometer at 79 N, *Radiat. Environ. Biophys.*, 48(2), 125–133, doi:10.1007/s00411-009-0219-y.
- Salminen, R., et al. (2005), Geochemical Atlas of Europe. Part 1: Background Information, Methodology and Maps, 526 pp., Espoo, Geol. Surv. of Finland.
- Sears, V. F. (1992), Neutron scattering lengths and cross sections, Neutron News, 3(3), 29–37, doi:10.1080/10448639208218770.
- Western, A. W., R. B. Grayson, and G. BlÖschl (2002), Scaling of soil moisture: A hydrologic perspective, *Annual Review of Earth and Planetary Sciences*, 30(1), 149–180, doi:10.1146/annurev.earth.30.091201.140434.
- Zacharias, S., et al. (2011), A network of terrestrial environmental observatories in Germany, *Vadose Zone J.*, 10, 955–973, doi:10.2136/vzi2010.0139.
- Zreda, M., D. Desilets, T. P. A. Ferré, and R. L. Scott (2008), Measuring soil moisture content non-invasively at intermediate spatial scale using cosmic-ray neutrons, *Geophys. Res. Lett.*, 35, L21402, doi:10.1029/2008GL035655.
- Zreda, M., W. J. Shuttleworth, X. Zeng, C. Zweck, D. Desilets, T. Franz, and R. Rosolem (2012), COSMOS: The COsmic-ray Soil Moisture Observing System, *Hydrol. Earth Syst. Sci.*, 16, 4079–4099, doi:10.5194/hess-16-4079-2012.
- Zweck, C., M. Zreda, and D. Desilets (2013), Snow shielding factors for cosmogenic nuclide dating inferred from Monte Carlo neutron transport simulations, *Earth Planet. Sci. Lett.*, 379, 64–71, doi:10.1016/j.epsl.2013.07.023.